



This document is a postprint version of an article published in Science of the Total Environment © Elsevier after peer review. To access the final edited and published work see <https://doi.org/10.1016/j.scitotenv.2019.06.448>

Document downloaded from:



Detection of *Ostreopsis cf. ovata* in environmental samples using an electrochemical DNA-based biosensor

Anna Toldrà^a, Carles Alcaraz^a, Jorge Diogène^a, Ciara K. O'Sullivan^{b,c*}, Mònica Campàs^{a*}

^aIRTA, Ctra. Poble Nou km 5.5, 43540 Sant Carles de la Ràpita, Tarragona, Spain

^bDepartament d'Enginyeria Química, Universitat Rovira i Virgili, Av. Països Catalans 26, 43007 Tarragona, Spain

^cInstitució Catalana de Recerca i Estudis Avançats (ICREA), Pg. Lluís Companys 23, 08010 Barcelona, Spain

* Corresponding authors: monica.campas@irta.cat; ciara.osullivan@urv.cat

Abstract

Given the increasing spread of toxic marine microalgae around the world, rapid, simple and low-cost detection tools are essential to protect human health and ecosystems. Herein, an electrochemical biosensor for the detection of *Ostreopsis cf. ovata*, a benthic microalgae known to produce palytoxins (PITXs), is described. The detection strategy involves isothermal recombinase polymerase amplification (RPA) of the target using tailed primers and a sandwich hybridisation assay on maleimide-coated magnetic beads immobilised on electrode arrays. The biosensor attained a limit of detection of 9 pg/μL of *O. cf. ovata* DNA (which corresponds to ~ 640 cells/L), with no interferences from two non-target *Ostreopsis* species (*O. cf. siamensis* and *O. fattorussoi*). The biosensor was applied to the analysis of planktonic and benthic environmental samples. Electrochemical *O. cf. ovata* DNA quantifications demonstrated an excellent correlation with other molecular methods and allowed the construction of a predictive regression model to estimate *O. cf. ovata* cell abundances. The performance of the biosensor demonstrates its potential implementation as an early warning tool in marine monitoring programs.

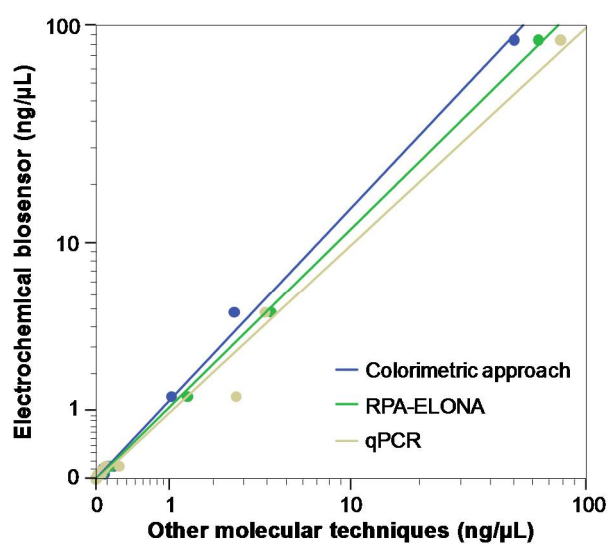
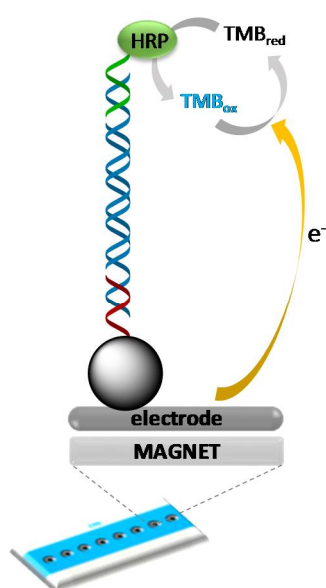
Keywords: marine microalgae; *Ostreopsis cf. ovata*; recombinase polymerase amplification (RPA); maleimide-coated magnetic bead (MB); electrochemical biosensor.

25 **Highlights:**

- 26
- 27
- 28
- 29
- 30
- First electrochemical biosensor for the detection of *Ostreopsis cf. ovata*
 - The biosensor combines isothermal amplification with magnetic beads as supports
 - The application of the biosensor to environmental samples is successfully proved
 - Excellent correlation with other molecular techniques and light microscopy
 - A rapid, simple and inexpensive alternative tool for marine monitoring is provided

31 **Graphical abstract:**

32



33 1. Introduction

34 Harmful algal blooms (HABs) include *Ostreopsis* species, a benthic microalgae known to produce palytoxin
35 (PITX)-like compounds. While initially reported in tropical and subtropical regions, *Ostreopsis* spp. have been
36 reported in more temperate regions such as the Mediterranean Sea (Mangialajo et al., 2011; Rhodes, 2011).
37 In this area, periodic summer blooms have been increasing during the last decade, where different *Ostreopsis*
38 species (*O. cf. ovata*, *O. cf. siamensis* and *O. fattorussoi*) have been described (Accoroni et al., 2016; Penna et
39 al., 2005), with *O. cf. ovata* being both the most toxic and the most widely distributed (Ciminiello et al., 2010).
40 Proliferations of *O. cf. ovata* have been involved in respiratory and skin distress in bathers, as well as in mass
41 mortalities of invertebrates (Berdalet et al., 2017; Mangialajo et al., 2011; Vila et al., 2016). Additionally, PITX-
42 like compounds have been found in seafood (Aligizaki et al., 2008; Amzil et al., 2012), thus representing a
43 potential risk to consumers.

44 HABs are natural phenomena that, realistically, cannot be eliminated. Nevertheless, monitoring programs can
45 significantly contribute to prevent and mitigate their impacts. In this sense, *Ostreopsis* spp. monitoring is
46 implemented in countries that regularly experience their negative effects, and is commonly performed using
47 light microscopy (Giussani et al., 2017; Vassalli et al., 2018). However, this method is time consuming and
48 based on morphology, which hampers correct microalgae identification, especially among *Ostreopsis* species.
49 Emerging molecular methods have demonstrated to provide faster and more accurate identification and
50 quantification of HABs than microscopy. PCR and quantitative PCR (qPCR) have been extensively applied to
51 several toxic microalgae and, specifically for *Ostreopsis* species, qPCR/PCR assays have been described for *O.*
52 *cf. ovata* (Battocchi et al., 2010; Casabianca et al., 2014; Perini et al., 2011), *O. cf. siamensis* (Battocchi et al.,
53 2010; Casabianca et al., 2013) and *O. fattorussoi* (Vassalli et al., 2018). Although qPCR is a good strategy for
54 the detection of HAB species, alternative user-friendly and *in-situ* molecular methods able to provide even
55 shorter analysis times and lower cost are highly desired.

56 Biosensors could address the needs of monitoring programs and, among them, electrochemical biosensors
57 stand out for several reasons: high sensitivity, short analysis times, simple and inexpensive instrumentation,
58 ease of handling, and compatibility with microfluidic systems and miniaturisation (Ronkainen et al., 2010). The
59 combination of these outstanding properties with the inherent nucleic acid specificity positions
60 electrochemical nucleic acid biosensors as attractive candidates for microalgae monitoring. However, there
61 are very few reports detailing electrochemical nucleic acid biosensors for microalgae detection. Such
62 biosensors commonly take advantage of a sandwich hybridisation format, where the target ribosomal RNA
63 (Diercks-Horn et al., 2011; Metfies et al., 2005) or DNA is sandwiched between an immobilised capture probe
64 and a labelled reporter probe. When targeting DNA, an amplification step is required prior to the
65 electrochemical detection. In this respect, a biosensor combining PCR amplification and electrochemical

66 detection was reported for microalgae detection (LaGier et al., 2007). However, PCR methodology relies on
67 thermal cycling, which hinders its implementation in miniaturised devices for *in-situ* testing.

68 Methods to isothermally amplify DNA have become increasingly popular due to the benefits of reducing
69 instrumental requirements and power consumption, thus being more suitable for *in-situ* analysis. Among
70 isothermal amplification methods, nucleic acid sequence-based amplification (NASBA) (Casper et al., 2004;
71 Loukas et al., 2017), loop-mediated isothermal amplification (LAMP) (Huang et al., 2017; Zhang et al., 2014),
72 rolling circle amplification (RCA) (Chen et al., 2015; Liu et al., 2019) and recombinase polymerase amplification
73 (RPA) (Toldrà et al., 2019; Toldrà et al., 2018) have been applied to microalgae detection. RPA is particularly
74 attractive due to its simplicity, high sensitivity, rapid amplification (~20-30 min), easy primer design as well as
75 its operation at low and constant temperature (~37-42 °C) (Lobato and O'Sullivan, 2018). To date, isothermal
76 amplification techniques have been successfully coupled with different detection techniques, including lateral
77 flow, fluorescence, turbidity and colorimetric readout. However, the combination of isothermal amplification
78 techniques with an electrochemical biosensor for the detection has never been reported for microalgae.

79 In our previous work, the combination of RPA with tailed primers for the colorimetric detection of *O. cf. ovata*
80 was described (Toldrà et al., 2019). Tailed primers consist of a single-stranded DNA (ssDNA) sequence (tail)
81 that is added to the species-specific primer using a C3 spacer, which prevents the formation of phosphodiester
82 bonds and further elongation, resulting in a double-stranded DNA (dsDNA) product flanked with ssDNA tails.
83 This facilitates the subsequent detection through a sandwich-type format assay using complementary
84 oligonucleotide probes: a thiolated capture probe and a labelled reporter probe. In this work, with the aim to
85 moving towards miniaturised and compact devices, we report an electrochemical biosensor for the detection
86 of *O. cf. ovata* that exploits RPA, tailed primers and maleimide-activated magnetic beads (MBs).
87 Oligocomplexes consisting of the RPA amplicon hybridised to a capture probe-functionalised MBs were
88 immobilised on a screen-printed carbon electrode array by magnetic capture and the resulting reduction
89 current was measured by amperometry (Fig. 1). A colorimetric approach was tested to demonstrate the
90 feasibility of the strategy prior to the biosensor development. The attainable LOD was determined using *O. cf.*
91 *ovata* genomic DNA and the specificity of the biosensor was evaluated using non-target *Ostreopsis* species (*O.*
92 *cf. siamensis* and *O. fattorussoi*). Additionally, the reusability of the electrodes and the stability of the capture
93 probe-functionalised MBs was studied. The biosensor was applied to the analysis of environmental samples,
94 and *O. cf. ovata* quantifications were compared with those obtained by qPCR, RPA-ELONA and light
95 microscopy.

96 **2. Materials and Methods**

97 **2.1. Reagents**

98 The TwistAmp Basic kit containing all enzymes and reagents necessary for the DNA amplification was obtained
99 from TwistDx Ltd. (Cambridge, UK). Custom DNA oligonucleotides were purchased from Biomers (Ulm,
100 Germany). PureCube maleimide-activated MagBeads (25 µm in diameter) were supplied by Cube Biotech
101 (Monheim, Germany). Tween-20, 3,3',5,5'-tetramethylbenzidine (TMB) liquid substrate, 6-mercapto-1-
102 hexanol, skimmed milk powder, bovine serum albumin (BSA) and all other reagents were acquired from Sigma-
103 Aldrich (Tres Cantos, Spain).

104 **2.2. Equipment**

105 Disruption of microalgae cells for subsequent DNA extraction was carried out using a BeadBeater-8 (BioSpec,
106 Bartlesville, USA). RPA reactions were performed in a Nexus Gradient Thermal Cycler (Eppendorf Ibérica, San
107 Sebastián de los Reyes, Spain). A NanoDrop 2000 spectrophotometer (Thermo Fisher Scientific, Madrid, Spain)
108 was used to quantitatively and qualitatively check extracted genomic DNA. Colorimetric measurements were
109 performed with a Microplate Reader KC4 (BIO-TEK Instruments, Inc., Winooski, USA) using Gen5 software to
110 collect data. Arrays of eight screen-printed electrodes (DRP-8x110) and a magnetic support (DRP-MAGNET8X)
111 were provided by Dropsens S.L. (Oviedo, Spain), and consist of 8 carbon working electrodes (2.5 mm in
112 diameter), each with its own carbon counter electrode and Ag/AgCl reference electrode. Electrochemical
113 measurements were performed using an 8-channel multiplexer PalmSens potentiostat (PalmSens BV, Houten,
114 The Netherlands) controlled by PalmSens PC software. A MagneSphere Technology Magnetic Separation Stand
115 (Promega Corporation, Madison, USA) was used for the magnetic separations.

116 **2.3. *Ostreopsis* cultures and environmental samples**

117 The present study employed genomic DNA extracted from: a) *Ostreopsis* cultures to perform the calibration
118 curves and specificity tests, and b) environmental samples to evaluate the applicability of the method. Strains
119 of *O. cf. ovata* (IRTA-SMM-16-133, MH790463), *O. cf. siamensis* (IRTA-SMM-16-84, MH790464) and *O.*
120 *fattorussoi* (IRTA-SMM-16-135: MH790465) were selected: *O. cf. ovata* as a positive control and *O. cf.*
121 *siamensis* and *O. fattorussoi* as negative controls. Additionally, 16 environmental samples (9 planktonic and 7
122 benthic samples) (Table S1) were collected in August 2017 at 9 stations along the Catalan coast (NW
123 Mediterranean Sea) and counted as described in Toldrà et al., 2019. Pellets from both *Ostreopsis* cultures and
124 50 mL-environmental samples were prepared by centrifugation (4500 rpm, 25 min) and stored at -20 °C.
125 Subsequent extraction of genomic DNA was carried out using a bead-beating system and the

126 phenol/chloroform/isoamylalcohol method. Extracted DNA samples (50 μ L) were quantified using a NanoDrop
127 and stored at -20 $^{\circ}$ C until RPA reaction.

128 **2.4. RPA reaction**

129 The primers used in this study include: one forward primer specific for *Ostreopsis* genus and one reverse
130 primer specific for *O. cf. ovata*. Primers amplified a fragment of 148 bp of the ITS1-5.8S ribosomal DNA gene
131 and were modified with oligonucleotide tails. Primers and probe sequences are listed in Table S2. RPA reaction
132 was performed at 37 $^{\circ}$ C for 30 min. Briefly, the RPA mixture was prepared by mixing 2.4 μ L of 10 μ M tailed
133 primers, 14.75 μ L of rehydration buffer, 22.95 μ L of molecular biology-grade water and 5 μ L of genomic DNA
134 extracted from: a) cultures of *O. cf. ovata* for the calibration curves (4-fold serial dilutions: from 10 to 0.002
135 ng/ μ L); b) cultures of *O. cf. siamensis* and *O. fattorusoi* for the the specificity study (1 ng/ μ L); and c)
136 environmental samples. 1/2 of lyophilised pellet was then added and the reaction was finally triggered by
137 addition of 2.5 μ L of 480 mM magnesium acetate to a final volume of 50 μ L. Positive controls and blanks (NTC
138 = no template control) were always included.

139 **2.5. Colorimetric and electrochemical detections**

140 Magnetic oligocomplexes were prepared as follows: 1) 10 μ L of maleimide-activated magnetic beads were
141 transferred to a tube; 2) 100 μ L of 500 nM thiolated capture probe in binding buffer (100 mM phosphate,
142 150 mM NaCl, pH 7.4) were added; 3) 100 μ L of 100 μ M 6-mercapto-1-hexanol in binding buffer were added
143 to block any non-functionalised maleimide groups; 4) 100 μ L of 5% w/v skimmed milk in binding buffer were
144 added to avoid non-specific adsorption and, finally, conjugates were re-suspended in 10 μ L of washing buffer.
145 When the amounts of MB varied, volumes were adjusted proportionally. Once the capture probe-MB
146 conjugates were prepared: 5) 4.5 μ L of conjugate were added to a new tube and placed on a magnetic stand
147 to remove the supernatant; 6) 45 μ L of RPA product and 45 μ L of binding buffer were incubated; 7) 90 μ L of
148 10 nM HRP-labelled reporter probe in 1% w/v BSA-washing buffer were added and 8) finally, conjugates were
149 re-suspended in 45 μ L of washing buffer. All steps were performed with agitation for 30 min at room
150 temperature, except for the capture probe conjugation step, which was incubated at 4 $^{\circ}$ C overnight. After
151 each step, conjugates were rinsed three times with 100 mM potassium phosphate, 150 mM NaCl, 0.05% v/v
152 Tween-20, pH 7.4, by placing the tube on the magnetic separation stand and removing the washing buffer.

153 For the colorimetric approach (to evaluate the feasibility of the strategy): 9) 10 μ L of the magnetic
154 oligocomplex suspension (equivalent to 10 μ L of RPA product) were placed into a new tube and the
155 supernatant was removed; 10) 125 μ L of TMB/H₂O₂ were incubated for 3 min; 11) tubes were placed on a
156 magnetic separator stand and 100 μ L were collected to read the absorbance at 620 nm.

157 For the electrochemical biosensor: 9) 10 μL of the magnetic oligocomplex suspension were placed on each
158 working electrode of the 8-electrode array with a magnetic support on the reverse side; the magnetic
159 oligocomplex was captured, and the supernatant was removed; 10) 10 μL of TMB/ H_2O_2 were added and
160 incubated for 3 min; 11) the reduction current was measured by amperometry after applying -0.2 V vs Ag/AgCl
161 for 4 s.

162 For the regeneration of the electrodes, the magnet was removed and the 8-electrode arrays were rinsed with
163 distilled water and air-dried. Fresh magnetic oligocomplexes were placed on the electrodes and the current
164 was again recorded. The process was repeated consecutively 10 times. To evaluate the storage stability, the
165 capture probe-coated MBs were prepared as described above, washed and aliquots were kept at 4 and -20 $^\circ\text{C}$.
166 Electrochemical signals were measured at day 0 (reference value) and at 7 and 17 days. Magnetic
167 oligocomplexes were obtained using 1 $\text{ng}/\mu\text{L}$ of *O. cf. ovata* genomic DNA in the RPA to both test the
168 reusability of electrodes and the stability storage of the MBs.

169 2.6. Data analysis

170 Colorimetric and electrochemical calibration curves were fitted to the sigmoidal logistic four-parameter
171 equation:

$$172 \quad y = y_0 + \frac{a}{1 + \left(\frac{x}{x_0}\right)^b}$$

173 where a and y_0 are the asymptotic maximum and minimum values, respectively, x_0 is the genomic
174 concentration (x) at the inflection point and b is the slope at the inflection point. The LOD was defined as the
175 blank plus three times its standard deviation (SD). All measurements were performed in triplicate. Curve
176 fittings were performed with SigmaPlot 12.0 (Systat Software Inc., California, USA).

177 Quantifications of 50-mL environmental samples obtained by the two approaches were expressed as $\text{ng}/\mu\text{L}$ of
178 *O. cf. ovata* in 50 μL of extracted DNA. Quantifications determined with the MB-based electrochemical
179 biosensor were compared with those obtained by the MB-based colorimetric method, as well as with those
180 obtained by RPA-ELONA and qPCR (Toldrà et al., 2019). Correlations were then analysed using Pearson's
181 correlation coefficient (r). To assess the relationship between electrochemical results and light microscopy cell
182 abundances, a quadratic polynomial regression model was developed for both benthic (cells/g fwm) and
183 planktonic (cells/L) samples. The correlation between predicted cell abundances from the electrochemical
184 tests and measured cell abundances from light microscopy counts was evaluated using Pearson's correlation
185 coefficient (r). IBM SPSS Statistics 23.0 (IBM Corp., New York, USA) was used for statistical analyses.

186 **3. Results and discussion**

187 **3.1. Colorimetric assay**

188 To demonstrate the feasibility of the strategy, the system was primarily tested using colorimetric detection.
189 After the sandwich-type assay on MBs, the analytical signal is proportional to the amount of HRP-labelled
190 reporter probe and, consequently, to the RPA amplicon concentration. In the colorimetric approach, the
191 enzymatic reaction between the HRP-labelled reporter probe and the enzymatic substrate (TMB/H₂O₂) was
192 performed in solution and the absorbance of the resulting product was measured.

193 The colorimetric calibration curve using different concentrations of *O. cf. ovata* genomic DNA was fitted to the
194 sigmoidal logistic four-parameter equation ($R^2 = 0.998$) (Fig. 2a). Relative standard deviations (RSD) were
195 below 14% (n=3), which indicated good assay reproducibility. An LOD of 10 pg/ μ L was attained, which
196 corresponds to 100 pg/sample (considering 50-mL samples and taking into account the DNA extraction, RPA
197 and detection protocols). Taking into account the amount of DNA per *O. cf. ovata* cell (Toldrà et al., 2019), the
198 LOD corresponds to ~800 cells/L.

199 **3.2. Electrochemical biosensor**

200 Once the strategy had been successfully demonstrated using the colorimetric assay, the resulting magnetic
201 oligocomplexes were integrated on an 8-electrode array to develop the biosensor. The enzymatic reaction
202 between the HRP-labelled reporter probe and the enzymatic substrate (TMB/H₂O₂) was carried out on the
203 electrode surface, and the TMB reduction current was subsequently measured using amperometry.

204 The electrochemical calibration curve achieved with the biosensor ($R^2 = 0.998$) is shown in Fig. 2b. The LOD
205 attained with the electrochemical biosensor was 9 pg/ μ L (90 pg/sample, ~640 cells/L), very similar to the one
206 achieved in the colorimetric approach and below the alarm thresholds established for *Ostreopsis* abundances.
207 In addition, the RSD of the biosensor was below 8.4% (n=3), demonstrating the high reproducibility of the
208 measurements. Surprisingly, high electrochemical signals (~3000 nA of NTC-subtracted maximum current
209 intensity, Fig. 2b) were obtained when the magnetic oligocomplexes were anchored on the electrode surface,
210 whereas lower current intensities (~1000 nA, *data not shown*) were recorded when performing the enzymatic
211 reaction in suspension and transferring the resulting oxidised TMB product (without MBs) to the electrodes.
212 To understand this difference in the signal, the electrochemical behaviour of bare MBs on the electrode
213 surface was studied using cyclic voltammetry. As reported by other authors (Baldrich et al., 2011), the
214 presence of MBs on the electrode showed a decrease in electron transfer (demonstrated by higher peak-to-
215 peak separation, lower peak currents, and lower charge) when compared to bare electrodes (Fig. S1). As a
216 consequence, the higher intensities registered with the biosensor are not due to the intrinsic properties of the

217 MBs but could be explained by the confinement of the oligocomplexes on the electrodes, which brings the
218 generation of oxidised TMB be closer to the transducer surface and its electrochemical detection less diffusion-
219 dependent.

220 The LODs provided by the MB-based colorimetric and electrochemical approaches are similar to those
221 reported for the colorimetric RPA-ELONA, where the sandwich assay is performed on maleimide plates instead
222 of on MBs. It is important to highlight that the methods described herein use approximately 5-fold less RPA
223 product as compared with the RPA-ELONA. If instead of using 10 μ L of oligocomplex, the whole amount from
224 the RPA reaction was used (45 μ L), amplified signals and improved LODs could be obtained. Although
225 compared to qPCR the LOD of the biosensor is almost 10-fold higher, the biosensor enables quantifications of
226 *O. cf. ovata* DNA below the current alarm thresholds. Moreover, it allows measurements to be performed in
227 a rapid and simple manner, paving the way towards its integration in a compact device and its true application
228 in the field, something more difficult to envisage with qPCR or colorimetric assays.

229 **3.3. Specificity study**

230 The final objective of the work is to apply the electrochemical biosensor to the analysis of environmental
231 samples. During the DNA extraction protocol of environmental samples, not only target DNA is extracted, but
232 also DNA from all organisms present in the sample. Consequently, it is necessary to ensure that the presence
233 of non-target microalgae species will not interfere in the biosensor performance causing false positive results.
234 With this aim, the specificity of the electrochemical biosensor for *O. cf. ovata* was evaluated using non-target
235 *Ostreopsis* species present in the Mediterranean (*O. cf. siamensis* and *O. fattorussoi*, which are taxonomically
236 close to *O. cf. ovata*) and comparing the current intensities with those obtained in the absence of target DNA
237 (NTC). No significant responses were obtained from the non-target *Ostreopsis* species (Fig. S2), indicating the
238 high specificity of the biosensor, which derives from the specificity of both the primers and the assay
239 configuration. Detection of *O. cf. ovata* without interferences from other taxonomically similar *Ostreopsis*
240 species present in the Mediterranean suggests therefore that the method is species-specific and should not
241 detect any other microalgae genus.

242 **3.4. Electrode array regeneration**

243 Screen-printed carbon electrodes are extensively used due to their low cost. Despite being originally designed
244 for single use, the possibility to re-use them and consequently reduce the biosensor cost was investigated. In
245 our strategy, oligonucleotides are not directly immobilised on the electrode surface as in most DNA-based
246 biosensors, but on MBs. The use of a magnetic field for immobilisation facilitates detachment of the magnetic
247 oligocomplexes from the electrode surface by simple magnet separation and subsequent facile removal of the
248 oligocomplexes from the electrode surface. Additionally, since all steps (immobilisation, blocking and

249 hybridisation), with the exception of electrochemical transduction are performed in solution, electrode fouling
250 is not likely to occur. With this purpose in mind, the possibility of electrode re-utilisation was evaluated.

251 Following the first electrochemical measurement, the magnet was removed and the electrodes were washed
252 with distilled water to remove the magnetic oligocomplexes. Subsequent cycles of magnetic
253 immobilisation/electrochemical measurement/cleaning resulted in responses close to 100 % (Fig. 3),
254 indicating not only that the magnetic oligocomplexes had been effectively removed from the electrodes, but
255 also that the electrodes had not suffered any damage. As expected, these results clearly demonstrate the re-
256 usability of the electrodes for at least 10 consecutive measurements.

257 **3.5. Stability of the functionalised MBs**

258 To investigate the possibility of shortening the protocol time, the storage stability of capture probe-
259 functionalised MBs at 4 and -20 °C was tested over 17 days. Electrochemical signals were constant at both
260 temperatures, demonstrating the real-time stability of the MBs with immobilized capture probes up to at least
261 17 days (Fig. S3). Additionally, such stability can be used to predict shelf life of DNA-coated MBs using the Q
262 Rule method (Anderson and Scott, 1991) according to the equation:

$$263 \quad \textit{predicted stability (time)} = \frac{\textit{real stability (time)}}{(Q10)^n}$$

264 where n is the temperature change divided by 10, and the value of Q10 is typically set at 2, 3, or 4, which
265 correspond to reasonable activation energies. In this work, taking into account that the functionalized MBs
266 are stable for at least 17 days, an n value of 2.4 and a conservative Q10 value of 2, the predicted stability of
267 the product at -20 °C is at least 3 months. This long-term stability of functionalised MBs significantly reduces
268 the assay time, as large amount of MBs can be prepared on the same day and stored until use.

269 **3.6. Analysis of environmental samples**

270 To demonstrate the applicability of the electrochemical biosensor, 16 environmental samples collected along
271 the Catalan coast were analysed. Sampling was performed in the summer period, when sea temperature
272 exceeds 24 °C and *Ostreopsis* proliferates, and included 4 locations (Table S1) where *Ostreopsis* blooms have
273 previously been reported: 2 locations in the south of the Catalan coast (Carnicer et al., 2015) and 2 locations
274 in the north of the Catalan coast (Vila et al., 2001). Specifically for the latter, *Ostreopsis* blooms have been
275 periodically associated with respiratory problems and skin irritations in humans. Environmental samples
276 included 9 seawater samples (planktonic samples) and 7 macroalgae samples (benthic samples). Although
277 *Ostreopsis* is a benthic genus that grow attached to macroalgae, *Ostreopsis* cells can be easily re-suspended in
278 the water column by mechanical action or hydrodynamic processes (Giussani et al., 2017). Consequently,
279 monitoring *Ostreopsis* cell abundances in water and on macroalgae is essential.

280 *Ostreopsis cf. ovata* DNA quantifications provided using the electrochemical biosensor were compared with
281 those provided by the colorimetric method, and previous results obtained by RPA-ELONA and qPCR (Table 1).
282 The samples contained a wide range of *O. cf. ovata* DNA concentrations, from undetected to 85.57 ng/ μ L.
283 From a qualitative point of view, most samples that provided negative results using the electrochemical
284 biosensor also gave negative results using other techniques, with the only exception being samples 1 and 13,
285 which were deemed positive using the more sensitive method of qPCR. As shown in Fig. 4, excellent
286 correlations were obtained when quantitatively comparing results of the techniques using RPA, both between
287 the electrochemical and colorimetric approaches (Pearson's $r = 0.998$; $P < 0.001$) and between the
288 electrochemical biosensor and RPA-ELONA ($r = 0.999$; $P < 0.001$). Similarly, good agreement was achieved
289 when comparing quantifications provided by the electrochemical biosensor and qPCR ($r = 0.993$; $P < 0.001$).

290 In order to evaluate the relationship between *O. cf. ovata* DNA quantification using the electrochemical
291 biosensor and light microscopy cell abundances, a quadratic polynomial regression model was constructed.
292 Although cells counted by light microscopy include all *Ostreopsis* species, they were identified as *O. cf. ovata*
293 after species-specific analysis using molecular methods. Additionally, environmental samples contained a
294 broad range of other microalgae genera at high abundances (Toldrà et al., 2019). When constructing the
295 model, samples that resulted negative for both electrochemistry and light microscopy (samples 15 and 16)
296 were not included, nor sample 1, which was considered as an outlier. The regression model was used to predict
297 cell abundances in the environmental samples from the biosensor DNA quantifications. The relationship
298 between the model-predicted and observed cell abundances was highly significant for both planktonic
299 (Pearson's $r = 0.932$; $P < 0.01$) and benthic (Pearson's $r = 0.975$; $P = 0.001$) samples (Fig. 5). This result indicates
300 that it is possible to correctly estimate *O. cf. ovata* cell concentrations from the developed biosensor in a range
301 below the alarm thresholds proposed for *Ostreopsis* cells (10000-30000 cells/L and 100000 cells/g fwm for
302 planktonic and benthic samples, respectively (Giussani et al., 2017; Vassalli et al., 2018)). Additionally, this
303 excellent correlation demonstrates the high specificity of the method, detecting *O. cf. ovata* without
304 interferences from other microalgae species present in the samples, even at much higher cell abundances.

305 **4. Conclusions**

306 In this work, the combination of the isothermal RPA technique using tailed primers with MBs as immobilisation
307 supports for the electrochemical detection of *O. cf. ovata* is described. Firstly, the use of RPA allows the
308 amplification of *O. cf. ovata* DNA without the need for thermal cycling, thus reducing power requirements.
309 Secondly, the use of tailed primers allows the detection of the amplified RPA product *via* a sandwich
310 hybridisation configuration. Finally, the use of maleimide-coated MBs as supports improves the assay kinetics
311 and enables reutilisation of the electrodes. Additionally, the stability of the capture probe immobilization
312 provides ready-to-use MBs, shortening the assay time.

313 Given the excellent analytical performance in terms of sensitivity, specificity, storage stability and good
314 correlation with other molecular methods as well as light microscopy, the implementation of this biosensor as
315 a quantitative and/or screening tool in routine microalgae monitoring programs is feasible. Additionally, it
316 offers great potential for subsequent integration in miniaturised devices, bringing it closer to in-field
317 deployment. This work thus constitutes a breakthrough in the development of rapid, simple, cost-effective
318 and easy-to-use analysis tools for the detection of toxic marine microalgae.

319 **Acknowledgements**

320 The research leading to these results has received funding from the Ministerio de Ciencia e Innovación through
321 the SEASENSING (BIO2014-56024-C2-2-R) and CIGUASENSING (BIO2017-87946-C2-2-R) projects. The authors
322 also acknowledge support from CERCA Programme/Generalitat de Catalunya. Anna Toldrà acknowledges
323 IRTA-Universitat Rovira i Virgili-Banco Santander for her PhD grant (2015PMF-PIPF-67).

324 **References**

- 325 Accoroni S, Romagnoli T, Penna A, Capellacci S, Ciminiello P, Dell'Aversano C, et al. *Ostreopsis fattorussoi* sp
326 nov (Dinophyceae), a new benthic toxic *Ostreopsis* species from the Eastern Mediterranean Sea.
327 Journal of Phycology 2016; 52: 1064-1084.
- 328 Aligizaki K, Katikou P, Nikolaidis G, Panou A. First episode of shellfish contamination by palytoxin-like
329 compounds from *Ostreopsis* species (Aegean Sea, Greece). Toxicon 2008; 51: 418-427.
- 330 Amzil Z, Sibat M, Chomerat N, Grossel H, Marco-Miralles F, Lemée R, et al. Ovatoxin-a and palytoxin
331 accumulation in seafood in relation to *Ostreopsis* cf. *ovata* blooms on the French Mediterranean coast.
332 Marine Drugs 2012; 10: 477-496.
- 333 Anderson G, Scott M. Determination of product shelf-life and activation-energy for 5 drugs of abuse. Clinical
334 Chemistry 1991; 37: 398-402.
- 335 Baldrich E, Gómez R, Gabriel G, Muñoz FX. Magnetic entrapment for fast, simple and reversible electrode
336 modification with carbon nanotubes: application to dopamine detection. Biosensors & Bioelectronics
337 2011; 26: 1876-1882.
- 338 Battocchi C, Totti C, Vila M, Masó M, Capellacci S, Accoroni S, et al. Monitoring toxic microalgae *Ostreopsis*
339 (dinoflagellate) species in coastal waters of the Mediterranean Sea using molecular PCR-based assay
340 combined with light microscopy. Marine Pollution Bulletin 2010; 60: 1074-1084.
- 341 Berdalet E, Tester PA, Chinain M, Fraga S, Lemée R, Litaker W, et al. Harmful algal blooms in benthic systems
342 recent progress and future research. Oceanography 2017; 30: 36-45.
- 343 Carnicer O, Guallar C, Andree KB, Diogène J, Fernández-Tejedor M. *Ostreopsis* cf. *ovata* dynamics in the NW
344 Mediterranean Sea in relation to biotic and abiotic factors. Environmental Research 2015; 143: 89-99.
- 345 Casabianca S, Casabianca A, Riobó P, Franco JM, Vila M, Penna A. Quantification of the toxic dinoflagellate
346 *Ostreopsis* spp. by qPCR assay in marine aerosol. Environmental Science & Technology 2013; 47: 3788-
347 3795.
- 348 Casabianca S, Perini F, Casabianca A, Battocchi C, Giussani V, Chiantore M, et al. Monitoring toxic *Ostreopsis*
349 cf. *ovata* in recreational waters using a qPCR based assay. Marine Pollution Bulletin 2014; 88: 102-109.
- 350 Casper ET, Paul JH, Smith MC, Gray M. Detection and quantification of the red tide dinoflagellate *Karenia brevis*
351 by real-time nucleic acid sequence-based amplification. Applied and Environmental Microbiology
352 2004; 70: 4727-4732.
- 353 Chen GF, Cai PP, Zhang CY, Wang YY, Zhang SB, Guo CL, et al. Hyperbranched rolling circle amplification as a
354 novel method for rapid and sensitive detection of *Amphidinium carterae*. Harmful Algae 2015; 47: 66-
355 74.
- 356 Ciminiello P, Dell'Aversano C, Dello Iacovo E, Fattorusso E, Forino M, Grauso L, et al. Complex palytoxin-like
357 profile of *Ostreopsis ovata*. Identification of four new ovatoxins by high-resolution liquid
358 chromatography/mass spectrometry. Rapid Communications in Mass Spectrometry 2010; 24: 2735-
359 2744.
- 360 Diercks-Horn S, Metfies K, Jackel S, Medlin LK. The ALGADEC device: a semi-automated rRNA biosensor for the
361 detection of toxic algae. Harmful Algae 2011; 10: 395-401.
- 362 Giussani V, Asnaghi V, Pedroncini A, Chiantore M. Management of harmful benthic dinoflagellates requires
363 targeted sampling methods and alarm thresholds. Harmful Algae 2017; 68: 97-104.
- 364 Huang HL, Zhu P, Zhou CX, He S, Yan XJ. The development of loop-mediated isothermal amplification combined
365 with lateral flow dipstick for detection of *Karlodinium veneficum*. Harmful Algae 2017; 62: 20-29.
- 366 LaGier MJ, Jack WFB, Goodwin KD. Electrochemical detection of harmful algae and other microbial
367 contaminants in coastal waters using hand-held biosensors. Marine Pollution Bulletin 2007; 54: 757-
368 770.

- 369 Liu FG, Chen GF, Zhang CY, Wang YY, Zhou J. Exponential rolling circle amplification coupled with lateral flow
370 dipstick strips as a rapid and sensitive method for the field detection of *Karlodinium veneficum*. Journal
371 of Applied Phycology 2019.
- 372 Lobato IM, O'Sullivan CK. Recombinase polymerase amplification: basics, applications and recent advances.
373 Trac-Trends in Analytical Chemistry 2018; 98: 19-35.
- 374 Loukas CM, McQuillan JS, Laouenan F, Tsaloglou MN, Ruano-Lopez JM, Mowlem MC. Detection and
375 quantification of the toxic microalgae *Karenia brevis* using lab on a chip mRNA sequence-based
376 amplification. Journal of Microbiological Methods 2017; 139: 189-195.
- 377 Mangialajo L, Ganzin N, Accoroni S, Asnaghi V, Blanford A, Cabrini M, et al. Trends in *Ostreopsis* proliferation
378 along the Northern Mediterranean coasts. Toxicon 2011; 57: 408-420.
- 379 Metfies K, Huljic S, Lange M, Medlin LK. Electrochemical detection of the toxic dinoflagellate *Alexandrium*
380 *ostentfeldii* with a DNA-biosensor. Biosensors & Bioelectronics 2005; 20: 1349-1357.
- 381 Penna A, Vila M, Fraga S, Giacobbe MG, Andreoni F, Riobó P, et al. Characterization of *Ostreopsis* and *Coolia*
382 (Dinophyceae) isolates in the western Mediterranean Sea based on morphology, toxicity and internal
383 transcribed spacer 5.8s rDNA sequences. Journal of Phycology 2005; 41: 212-225.
- 384 Perini F, Casabianca A, Battocchi C, Accoroni S, Totti C, Penna A. New approach using the real-time PCR method
385 for estimation of the toxic marine dinoflagellate *Ostreopsis cf. ovata* in marine environment. Plos One
386 2011; 6: 9.
- 387 Rhodes L. World-wide occurrence of the toxic dinoflagellate genus *Ostreopsis* Schmidt. Toxicon 2011; 57: 400-
388 407.
- 389 Ronkainen NJ, Halsall HB, Heineman WR. Electrochemical biosensors. Chemical Society Reviews 2010; 39:
390 1747-1763.
- 391 Toldrà A, Alcaraz C, Andree KB, Fernández-Tejedor M, Diogène J, Katakis I, et al. Colorimetric DNA-based assay
392 for the specific detection and quantification of *Ostreopsis cf. ovata* and *Ostreopsis cf. siamensis* in the
393 marine environment. Harmful Algae 2019; 84: 27-35.
- 394 Toldrà A, Jauset-Rubio M, Andree KB, Fernández-Tejedor M, Diogène J, Katakis I, et al. Detection and
395 quantification of the toxic marine microalgae *Karlodinium veneficum* and *Karlodinium armiger* using
396 recombinase polymerase amplification and enzyme-linked oligonucleotide assay. Analytica Chimica
397 Acta 2018; 1039: 140-148.
- 398 Vassalli M, Penna A, Sbrana F, Casabianca S, Gjerci N, Capellacci S, et al. Intercalibration of counting methods
399 for *Ostreopsis* spp. blooms in the Mediterranean Sea. Ecological Indicators 2018; 85: 1092-1100.
- 400 Vila M, Abós-Herràndiz R, Isern-Fontanet J, Àlvarez J, Berdalet E. Establishing the link between *Ostreopsis cf.*
401 *ovata* blooms and human health impacts using ecology and epidemiology. Scientia Marina 2016; 80:
402 107-115.
- 403 Vila M, Garcés E, Masó M. Potentially toxic epiphytic dinoflagellate assemblages on macroalgae in the NW
404 Mediterranean. Aquatic Microbial Ecology 2001; 26: 51-60.
- 405 Zhang FY, Shi YH, Jiang KJ, Song W, Ma CY, Xu ZL, et al. Rapid detection and quantification of *Prorocentrum*
406 *minimum* by loop-mediated isothermal amplification and real-time fluorescence quantitative PCR.
407 Journal of Applied Phycology 2014; 26: 1379-1388.
- 408

Table 1 *O. cf. ovata* DNA quantifications (ng/ μ L) of 16 environmental samples (planktonic and benthic) provided by the electrochemical MB-based biosensor and the colorimetric MB-based assay (mean \pm SD, $n = 3$). Quantifications obtained by RPA-ELONA and qPCR are shown (Toldrà et al., 2019).

Sample number	<i>O. cf. ovata</i> DNA (ng/ μ L)			
	Electrochemical	Colorimetric	RPA-ELONA	qPCR
Sample 1	nd	nd	nd	0.010 \pm 0.002
Sample 2	85.573 \pm 8.968	50.516 \pm 1.870	63.721 \pm 11.896	78.781 \pm 6.367
Sample 3	nd	nd	nd	nd
Sample 4	nd	nd	nd	nd
Sample 5	0.086 \pm 0.008	0.081 \pm 0.011	0.083 \pm 0.033	0.063 \pm 0.021
Sample 6	1.299 \pm 0.420	1.045 \pm 0.218	1.369 \pm 0.185	2.748 \pm 0.248
Sample 7	0.132 \pm 0.037	0.110 \pm 0.006	0.149 \pm 0.069	0.098 \pm 0.016
Sample 8	0.039 \pm 0.005	0.031 \pm 0.008	0.025 \pm 0.011	0.019 \pm 0.001
Sample 9	0.047 \pm 0.016	0.082 \pm 0.040	0.064 \pm 0.024	0.056 \pm 0.022
Sample 10	0.102 \pm 0.031	0.071 \pm 0.002	0.082 \pm 0.016	0.083 \pm 0.021
Sample 11	0.035 \pm 0.015	0.038 \pm 0.012	0.020 \pm 0.005	0.022 \pm 5E-05
Sample 12	0.132 \pm 0.033	0.185 \pm 0.045	0.139 \pm 0.042	0.250 \pm 0.009
Sample 13	nd	nd	nd	0.005 \pm 2E-04
Sample 14	4.403 \pm 1.042	2.686 \pm 0.321	4.220 \pm 0.855	3.918 \pm 0.257
Sample 15	nd	nd	nd	nd
Sample 16	nd	nd	nd	nd

nd: not detected

Figure 1 Schematic illustration of the electrochemical biosensor.

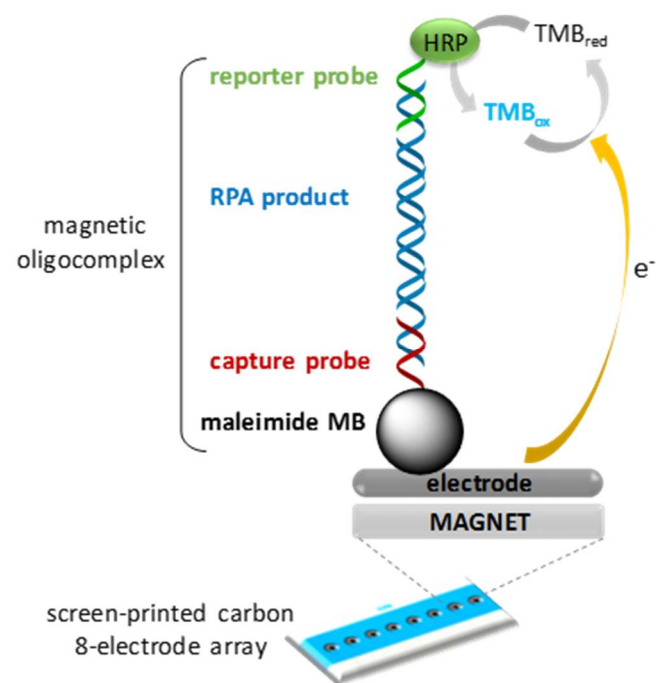


Figure 2 Calibration curves obtained using different concentrations of *O. cf. ovata* genomic DNA: (a) colorimetric assay and (b) electrochemical biosensor. Error bars are the standard deviation of the mean, $n = 3$.

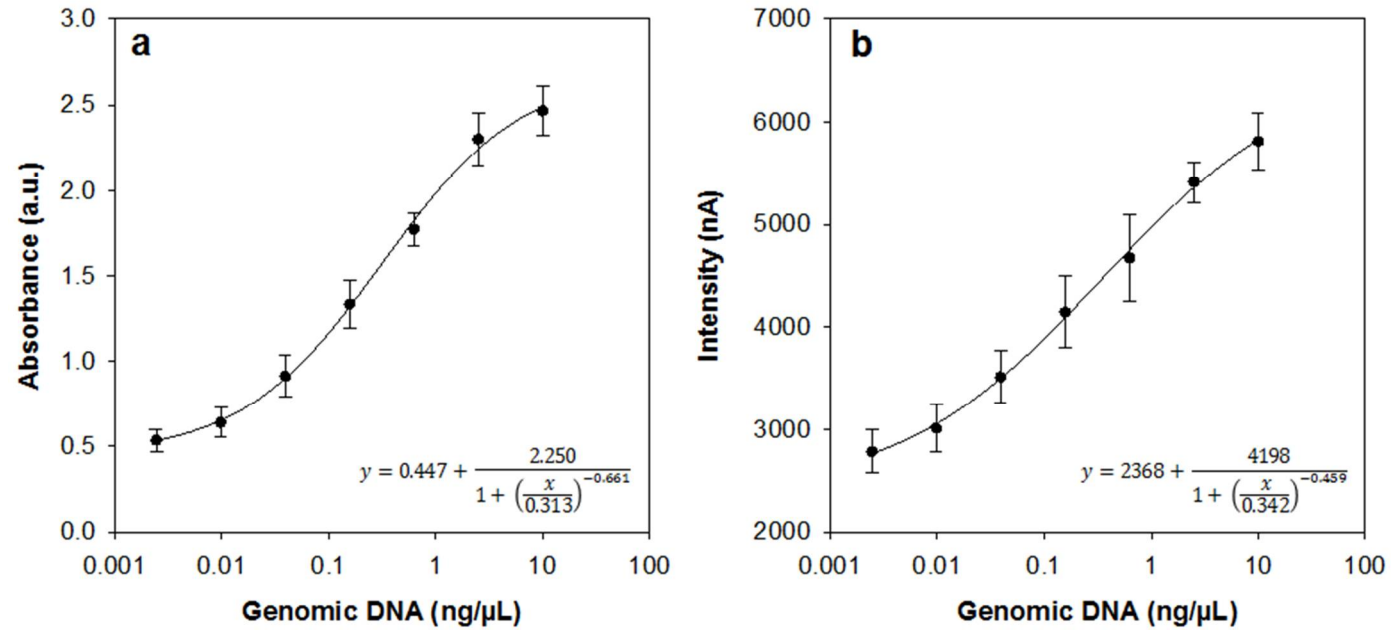


Figure 3 Electrochemical responses of the electrochemical biosensor after 10 cycles of magnetic immobilisation/electrochemical measurement/cleaning. Error bars are the standard deviation of the mean, $n = 3$.

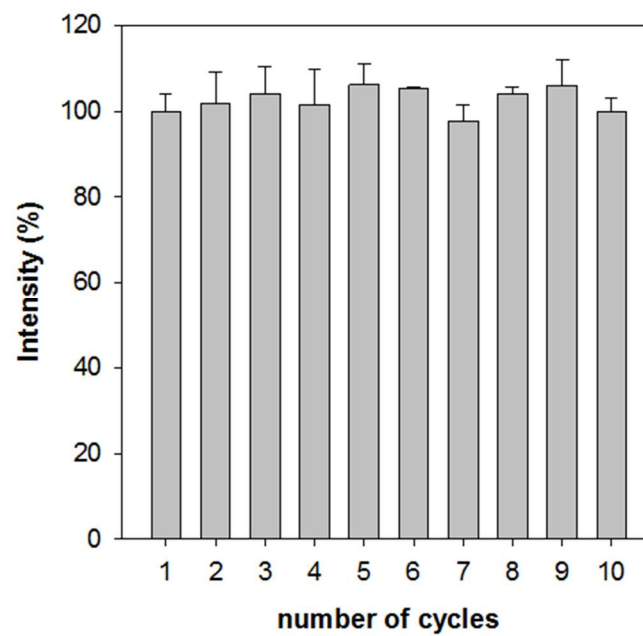


Figure 4 Correlation between *O. cf. ovata* DNA quantifications provided by the electrochemical biosensor and those obtained by the colorimetric assay, RPA-ELONA and qPCR in all examined environmental samples.

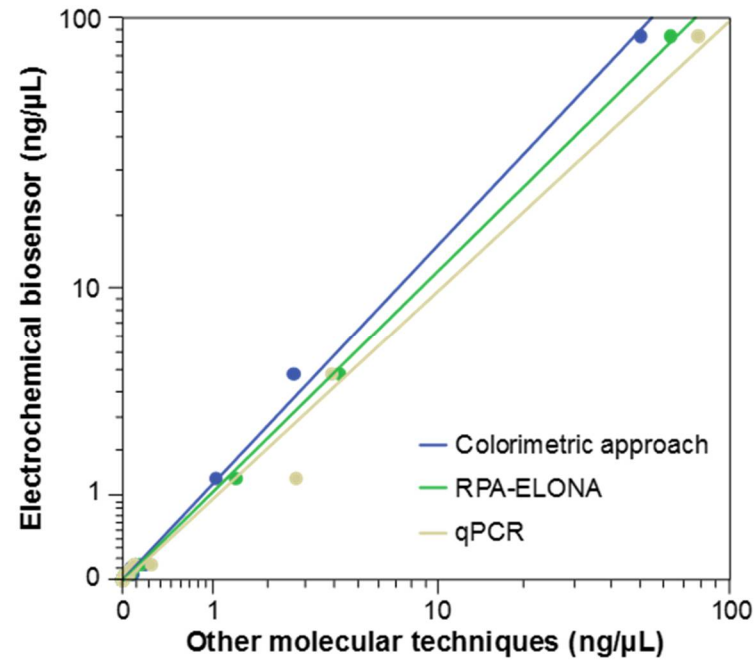


Figure 5 Relationship between predicted cell abundances provided by the regression model and those counted by light microscopy in: (a) planktonic samples (cells/L) and (b) benthic samples (cells/g fwm). Pearson's correlation coefficient is shown.

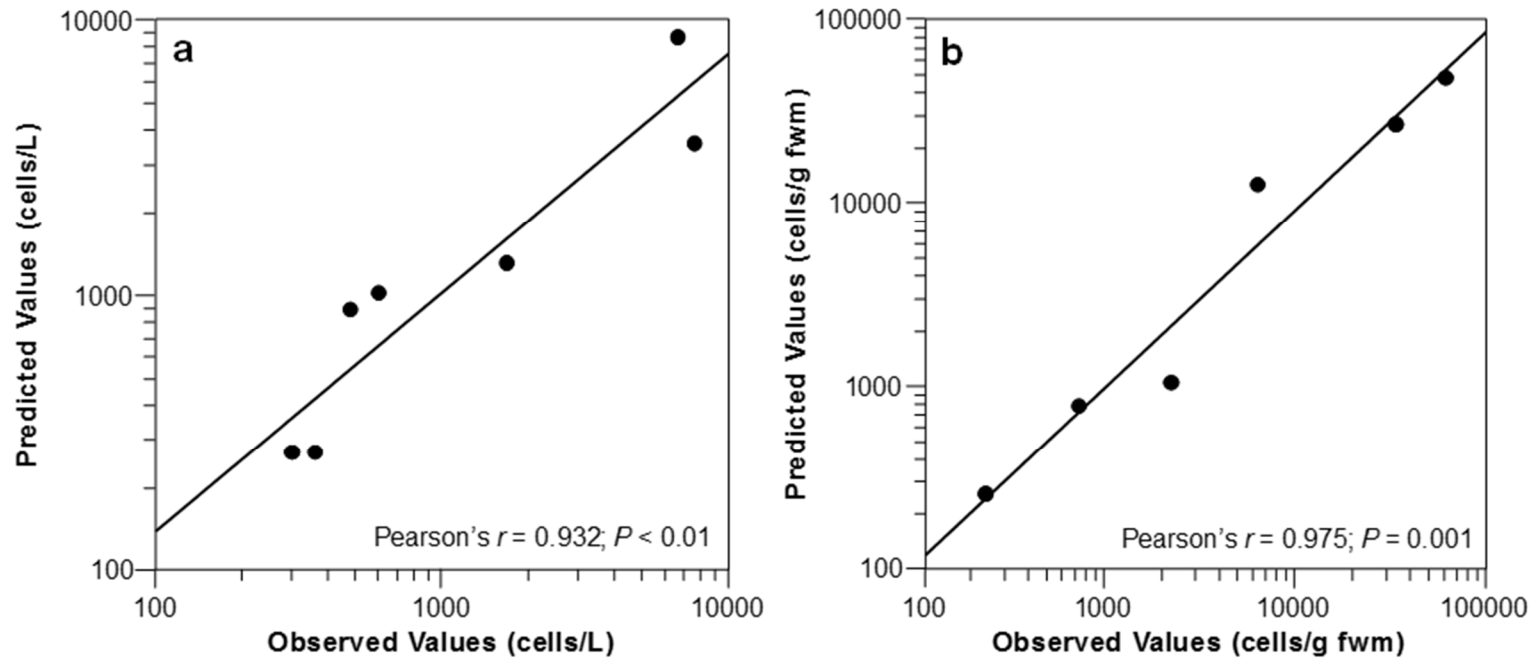


Table S1. Environmental samples collected in August 2017 along the Catalan coast. Location and geographical coordinates of the sampling stations as well as *Ostreopsis* spp. abundances obtained by light microscopy for planktonic (cells/L) and benthic (cells/g fwm) samples are shown. Data obtained from (*).

Sample number	Sample type	Locality	Station number	Geographical coordinates	<i>Ostreopsis</i> spp. cell abundances
Sample 1	planktonic	Palamós, La Fosca	1	N 41°51'20.71" E 3°8'32.01"	2840
Sample 2	benthic	Palamós, La Fosca	1	N 41°51'20.71" E 3°8'32.01"	60710
Sample 3	planktonic	Palamós, La Fosca	2	N 41°51'28.18" E 3°8'39.84"	360
Sample 4	benthic	Palamós, La Fosca	2	N 41°51'28.18" E 3°8'39.84"	210
Sample 5	planktonic	Sant Andreu de Llavaneres	3	N 41°33'7.69" E 2°29'31.66"	7600
Sample 6	benthic	Sant Andreu de Llavaneres	3	N 41°33'7.69" E 2°29'31.66"	32831
Sample 7	planktonic	Sant Andreu de Llavaneres	4	N 41°33'12.25" E 2°29'45.20"	6620
Sample 8	planktonic	Sant Andreu de Llavaneres	5	N 41°33'17.06" E 2°29'54.47"	600
Sample 9	planktonic	L'Ametlla de Mar	6	N 40°52'28.35" E 0°47'43.67"	1680
Sample 10	benthic	L'Ametlla de Mar	6	N 40°52'28.35" E 0°47'43.67"	667
Sample 11	planktonic	L'Ametlla de Mar	7	N 40°50'47.90" E 0°45'44.04"	480
Sample 12	benthic	L'Ametlla de Mar	7	N 40°50'47.90" E 0°45'44.04"	2071
Sample 13	planktonic	Les Cases d'Alcanar	8	N 40°32'1.00" E 0°31'7.24"	300
Sample 14	benthic	Les Cases d'Alcanar	8	N 40°32'1.00" E 0°31'7.24"	6015
Sample 15	planktonic	Les Cases d'Alcanar	9	N 40°33'15.71" E 0°31'58.71"	nd
Sample 16	benthic	Les Cases d'Alcanar	9	N 40°33'15.71" E 0°31'58.71"	nd

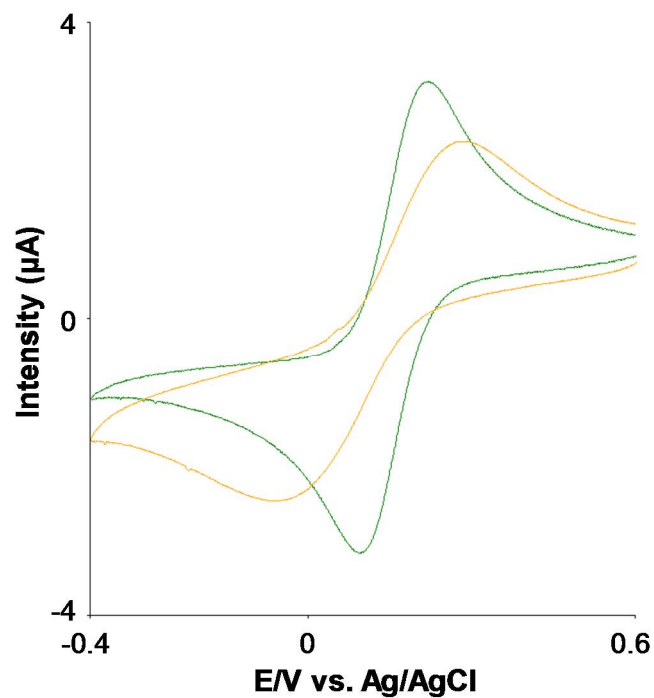
nd: not detected

(*) Toldrà A, Alcaraz C, Andree KB, Fernández-Tejedor M, Diogène J, Katakis I, et al. Colorimetric DNA-based assay for the specific detection and quantification of *Ostreopsis* cf. *ovata* and *Ostreopsis* cf. *siamensis* in the marine environment. Harmful Algae 2019; 84: 27-35.

Table S2. List of primers (underlined) and probes and their respective modifications.

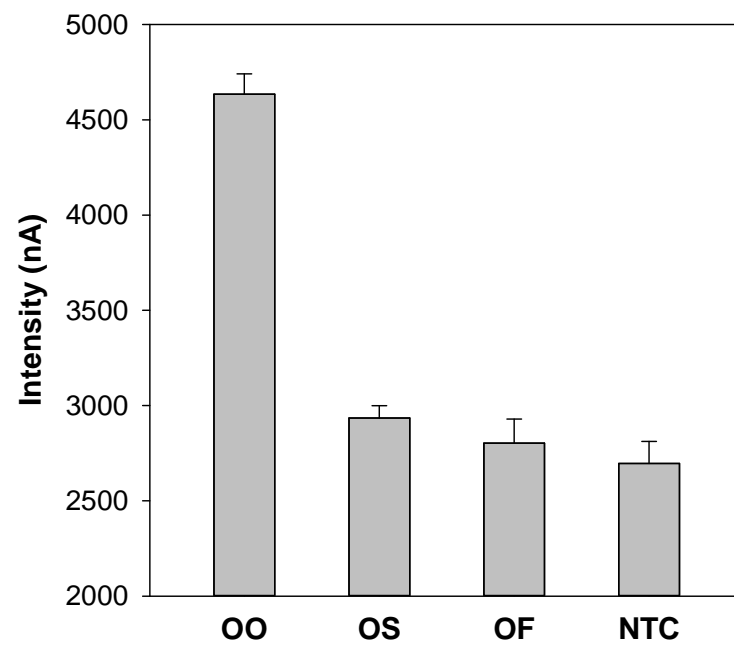
Name	Sequence (5'-3')
Forward <i>O. cf. ovata</i> primer with tail	gtt ttc cca gtc acg ac-C3- <u>aca atg ctc atg cca atg atg ctt gg</u>
Reverse <i>Ostreopsis</i> spp. primer with tail	tgt aaa acg acg gcc agt-C3- <u>gca wtt ggc tgc act ctt cat aty gt</u>
<i>O. cf. ovata</i> capture probe	gtc gtg act ggg aaa act ttt ttt ttt tt-C3-SH
Reporter probe	HRP-act ggc cgt cgt ttt aca

Fig. S1. Cyclic voltammograms (CVs) and analytical parameters obtained using a bare screen-printed electrode (green line) and a MB-modified screen-printed electrode (orange line). CVs were performed using 10 μL of 1 mM $[\text{Fe}(\text{CN})_6]^{3-/4-}$ (in 0.1 M phosphate buffer solution with 0.1 M KCl, pH 7.2.) at a scan rate of 50 mV/s. 1 μL of malimide-activated MBs were used, which corresponds to 10 μL of oligocomplex.



	E_{ox} (V)	E_{red} (V)	ΔE (V)	Height E_{ox} (μA)	Height E_{red} (μA)	Charge E_{ox} (μC)	Charge E_{red} (μC)
Bare electrode	0.221	0.093	0.128	3.103	-3.180	1.170	-1.142
MB-modified electrode	0.291	-0.054	0.345	1.965	-1.752	0.928	0.920

Fig. S2. Electrochemical responses of the electrochemical biosensor using DNA from: *O. cf. ovata* (OO), *O. cf. siamensis* (OS), *O. fattorusoi* (OF) and no template control (NTC). Error bars are the mean standard deviation, $n = 3$.



Fig, S3, Electrochemical responses corresponding to the stability study of functionalized MBs stored at 4 °C (black bars) and at -20 °C (grey bars), respect to day 0 (white bar, reference value). Error bars are the standard deviation of the mean, $n = 3$.

